CFTR Regulation of Intracellular pH and Ceramides Is Required for Lung Endothelial Cell Apoptosis

Julie Noe[1], Daniela Petrusca[2], Natalia Rush[2], Ping Deng[3], Mary VanDemark[2], Evgeny Berdyshev[4], Yuan Gu[2], Patricia Smith[2], Kelly Schweitzer[2], Joseph Pilewsky[6], Viswanathan Natarajan[5], Zao Xu[3], Alexander G. Obukhov[4], and Irina Petrache[2]

[1]Section of Pulmonology and Critical Care, Department of Pediatrics, [2]Division of Pulmonary, Allergy, Critical Care and Occupational Medicine, [3]Department of Anatomy, and the [4]Department of Cellular and Integrative Physiology, Indiana University, Indianapolis, Indiana; [5]Division of Pulmonary and Critical Care Medicine, University of Chicago, Chicago, Illinois; and [6]Division of Pulmonary and Critical Care Medicine, University of Pittsburgh, Pittsburgh, Pennsylvania

The functional significance of the expression of cystic fibrosis transmembrane regulator (CFTR) on endothelial cells has not yet been elucidated. Since CFTR has been implicated in the regulation of intracellular sphingolipid levels, which are important regulators of endothelial cell apoptosis in response to various insults, we investigated the role of CFTR in the apoptotic responses of lung endothelial cells. CFTR was detected as a functional chloride channel in primary lung endothelial cells isolated from both pulmonary arteries (human or mouse) and bronchial arteries (sheep). Both specific CFTR inhibition with 2-(phenylamino) benzoic acid diphenylamine-2-carboxylic acid, 5-[(4-carboxyphenyl)methylene]-2-thioxo-3-[(3-trifluoromethyl)phenyl-4-thiazolidinone ($CFTR_{inh}$-172), or 5-nitro-2-(3-phenylpropylamino)benzoic acid and CFTR knockdown significantly attenuated endothelial cell apoptosis induced by staurosporine or H_2O_2. $CFTR_{inh}$-172 treatment prevented the increases in the ceramide:sphingosine-1 phosphate ratio induced by H_2O_2 in lung endothelial cells. Replenishing endogenous ceramides via sphingomyelinase supplementation restored the susceptibility of CFTR-inhibited lung endothelial cells to H_2O_2-induced apoptosis. Similarly, the anti-apoptotic phenotype of CFTR-inhibited cells was reversed by lowering the intracellular pH, and was reproduced by alkalinization before H_2O_2 challenge. TUNEL staining and active caspase-3 immunohistochemistry indicated that cellular apoptosis was decreased in lung explants from patients with cystic fibrosis compared with those with smoking-induced chronic obstructive lung disease, especially in the alveolar tissue and vascular endothelium. In conclusion, CFTR function is required for stress-induced apoptosis in lung endothelial cells by maintaining adequate intracellular acidification and ceramide activation. These results may have implications in the pathogenesis of cystic fibrosis, where aberrant endothelial cell death may dysregulate lung vascular homeostasis, contributing to abnormal angiogenesis and chronic inflammation.

Keywords: cystic fibrosis; vascular; sphingolipids; cell death; pulmonary artery; bronchial artery; oxidative stress

CLINICAL RELEVANCE

This work is important in the understanding of cystic fibrosis pathogenesis as well as in the more general area of vascular responses to oxidative stress, as it reveals mechanisms by which the cystic fibrosis transmembrane conductance regulator regulates lung endothelial cell apoptosis induced by oxidative stress.

The most common cause of death in cystic fibrosis (CF) is respiratory failure from progressive lung disease characterized by thickened airway secretions accompanied by chronic respiratory infections and chronic inflammatory changes. The molecular defect involved in CF is the mutated cystic fibrosis transmembrane conductance regulator (CFTR), a plasma membrane cAMP-dependent chloride channel (1). CFTR mutations cause absent, reduced numbers, or poorly functioning ion channels on the cell membrane, which impair the cell's ability to move chloride and bicarbonate into the extracellular space. These alterations in the CFTR expressed on pulmonary airway epithelial cells lead to the accumulation of abnormally thickened respiratory secretions in CF. However, CFTR is expressed in other resident cells in the lung, including pulmonary microvascular endothelial cell (2) and pulmonary artery smooth muscle cells (3). While the role of CFTR in epithelial cell function has been the subject of extensive research, its role in the function of other cellular compartments in the lung is largely unknown. Since endothelial cells constitute an important defense barrier with an active role in regulating inflammatory responses in the lung, elucidating the role of CFTR in the endothelium may uncover mechanisms that underlie the chronic inflammatory responses in CF lungs. We set out to investigate the role of CFTR in lung endothelial cells, in particular in the regulation of cell death (select data were presented in abstract form [4]).

Lung endothelial cell programmed cell death, or apoptosis, is a highly regulated process that is required for normal blood vessel formation and for orderly removal of senescent, injured, and infected cells from tissues. A dysregulated or impaired apoptotic process may, however, trigger inflammatory responses (5) and contribute to increased morbidity in response to respiratory infectious agents such as *Pseudomonas aeruginosa* (6). In lung epithelial cells, disruption of CFTR function has been shown to both inhibit (7, 8) and augment apoptosis (9). Abnormalities in intracellular acidification and alterations of ceramide levels have been implicated in both the anti- and pro-apoptotic effects of CFTR inhibition (8, 9). The effect of CFTR inhibition on endothelial cell apoptosis or sphingolipid signaling is not known.

The sphingolipids ceramide and sphingosine-1 phosphate (S1P) are signaling mediators involved in the regulation of lung epithelial and endothelial cell apoptosis and survival, respectively (9–12). CFTR, an ATP-binding cassette transporter localized in ceramide-rich membrane microdomains, has been involved in the regulation of sphingolipid, particularly S1P, transport across the plasma membrane (13). Furthermore, the

(*Received in original form July 16, 2008 and in final form December 11, 2008*)

This work was supported by CF: Clinical fellowship training grant: 4486408 (to J.N.) and by the NIH-NHLBI (contract grant number: R01 HL 077328 [to I.P.] and R0179396 [to V.N.]).

Correspondence and requests for reprints should be addressed to Irina Petrache, M.D., Indiana University, Division of Pulmonary, Allergy, Critical Care and Occupational Medicine, Van Nuys Medical Science Building, 635 Barnhill Drive, MS224, Indianapolis, IN 46202-5120. E-mail: ipetrach@iupui.edu

This article has an online supplement, which is accessible from this issue's table of contents at www.atsjournals.org

Am J Respir Cell Mol Biol Vol 41. pp 314–323, 2009
Originally Published in Press as DOI: 10.1165/rcmb.2008-0264OC on January 23, 2009
Internet address: www.atsjournals.org

inability of CFTR-inhibited cells to generate optimal intracellular acidification may impair the activity of the acid sphingomyelinase or ceramidases, enzymes involved in the control of intracellular ceramide levels. Since endothelial cells are susceptible to oxidative stress–induced ceramide-dependent apoptosis, we studied the role of CFTR in H_2O_2-induced apoptosis of primary endothelial cells isolated from pulmonary and bronchial arteries. Utilizing specific pharmacologic tools, we identified an inability of the CFTR-inhibited endothelium to augment ceramides in response to stress, concomitant with a pH-dependent impairment in apoptosis.

MATERIALS AND METHODS

Chemicals and Reagents

All chemicals were purchased from Sigma Aldrich (St. Louis, MO) unless otherwise stated.

Cells

Mouse lung endothelial cells were generously provided by Dr. Patty Lee (Yale University, New Haven, CT). Sheep primary bronchial artery endothelial cells were generously provided by Dr. Elizabeth Wagner (The Johns Hopkins University, Baltimore, MD). Human lung microvascular endothelial cells (HLMVEC) were obtained from Lonza (Allendale, NJ) and maintained in culture medium consisting of EMB-2, 10% FBS, 0.4% hydrocortisone, 1.6% hFGF, 1% VEGF, 1% IGF-1, 1% ascorbic acid, 1% hEGF, 1% GA-100, and 1% heparin. All primary cell cultures were maintained at 37°C in 5% CO_2 and 95% air. Experiments were performed up to passage 10 with cells at 80 to 100% confluence.

Cellular Toxicity and Viability

Cellular toxicity and viability in response to treatments with pharmacologic CFTR and non-CFTR chloride channel inhibitors was determined by measuring LDH release (Promega, Madison, WI) in endothelial cells at 30 min and 18 h after treatment, using the manufacturer's protocol.

CFTR Inhibitory Studies

Endothelial cells were treated with the following specific CFTR channel blockers: 2-(phenylamino)benzoic acid diphenylamine-2-carboxylic acid (DPC) (200 μM in ethanol vehicle; the final ethanol concentration in cell culture media was 2%), 5-nitro-2-(3-phenylpropylamino)benzoic acid (NPPB) (200 μM in ethanol, 5%), and 5-[(4-carboxyphenyl)methylene]-2-thioxo-3-[(3-trifluoromethyl)phenyl-4-thiazolidinone ($CFTR_{inh}$-172) (20 μM in DMSO, 0.2%); and the specific non-CFTR chloride channel inhibitor disodium 4,4′-diisothiocyanatostilbene-2,2′-disulfonate (DIDS) (200 μM in H_2O). Cell growth media were replaced with serum-free media for 2 hours before the addition of inhibitors. Cells were pretreated with these inhibitors for 1 hour before treatments with staurosporine or H_2O_2.

In addition, CFTR was knocked down via CFTR-specific siRNA (Ambion, Austin, TX), using a nontarget siRNA (scramble and siGlo from Ambion) as a control. Cells were transfected with 25 to 100 nM siRNA using a siPORT FX transfection kit (Ambion). Cells were treated staurosporine or vehicle after 72 hours and lysates were obtained for real-time PCR or caspase-3 activity quantification.

Patch Clamp Analysis of CFTR Channel

Recording electrodes were prepared from borosilicate glass using a horizontal electrode puller (P-97; Sutter Instruments, Novato, CA) to produce tip openings of 1 to 2 μm (3–5 MΩ). Electrodes were filled with an intracellular solution containing (in mM): 43 CsCl, 92 $CsMeSO_4$, 5 TEA, 2 EGTA, 1 $MgCl_2$, 10 HEPES, 2 Mg-ATP, and 0.4 Na-GTP, pH 7.2, 295 to 300 mOsm/L. The extracellular solution contained (in mM): 6 KCl, 144 NaCl, 1 $MgCl_2$, 1 $CaCl_2$, 10 HEPES, and 10 Glucose, pH 7.2, 290 to 300 mOsm/L. The flow rate was 2 to 3 ml/minute. Coverslips with endothelial cells were placed in a recording chamber, and the cells were visualized with an infrared-differential interference contrast microscope (BX50WI; Olympus, Center Valley, PA) and CCD camera. Whole-cell voltage-clamp recordings were performed at 24°C with an Axopatch 200B amplifier (Axon Instruments, Sunnyvale, CA). After tight-seal (> 1 GΩ) formation, the electrode capacitance was compensated. The membrane capacitance, series resistance and input resistance of the recorded endothelial cells were measured by applying a 5 mV (10 ms) hyperpolarizing voltage pulse from a holding potential of 0 mV. Cells with a series resistance change greater than 15% during the experiment were excluded from the analysis. Signals were filtered at 5 kHz and digitized at a sampling rate of 10 kHz using a data-acquisition program (Axograph 4.6). At a holding potential of 0 mV, the CFTR currents were evoked by voltage steps (from −150 mV to +80 mV in 10-mV increments, 1 s). The activators and blockers of CFTR were applied in the bath solution at the indicated concentrations.

In a separate set of experiments, where we studied ion currents in cultured lung endothelial cells treated with H_2O_2 in the presence and absence of the $CFTR_{inh}$-172 inhibitor, the currents were measured 2 minutes after the rupture of the cell membrane to allow the exchange of the cytosol for the pipette solution. The standard extracellular solution contained (mM): 145 NaCl, 2.5 KCl, 1 $MgCl_2$, 2 $CaCl_2$, 5.5 Glucose, and 10 HEPES (pH 7.2), whereas the intracellular solution contained (mM): 140 $CsMeSO_3$, 10 CsCl, 2 $MgCl_2$, 0.5 EGTA, and 10 HEPES (pH 7.2). The osmolarity of recording solutions was adjusted to 295 to 300 mOsm with mannitol, if needed. The currents were recorded during 400-millisecond step pulses to −100 mV and +100 mV from the holding potential of 0 mV using the Optopatch amplifier (Cairn Research Ltd, Kent, UK) and digitized with the Digidata 1322A AD converter (Molecular Probes). The Clampfit 10 software (Molecular Probes) was used for data analysis. The mean cell capacitance (± SD) of untreated cells was 19.6 ± 7.3 pF.

Polymerase Chain Reaction

Total RNA was extracted from cultured cells using a commercial total RNA isolation kit (Qiagen, Valencia, CA), and the cDNA was reversely transcripted from 1 μg of total RNA by using the first-strand synthesis kit (Invitrogen, Carlsbad, CA) with random primers. The cDNA products were amplified by an RT-PCR module using synthesized primers for CFTR gene as target gene and GAPDH primers for the GAPDH gene as reference gene. The primers used for the gene amplification were synthesized by Invitrogen. Primers for human CFTR gene were (accession number: NM_000492): forward, 5-GCA TTTGCTGATTGCACAGT-3; reverse, 5-ACTGCCGCACTTT GTTCTCT-3. Primers for the ovine CFTR (accession number: NM_001009781) were: forward, 5-cctttccaacaacctgaacaa-3; reverse, 5-aggactacgaggaaagcaagc-3. Primers for the human and ovine GAPDH gene as reference gene were: forward, 5-GCATTTGCTGATTGCA CAGT-3; reverse, 5-ACTGCCGCACTTTGTTCTCT-3). The RT-PCR products were electrophoresed on a 1.5% TAE agarose gel, and the bands for human and ovine CFTR were detected at a size of 100 bp and 150 bp, respectively. The bands were excised and the product was checked by sequencing at the Indiana University Genetics Core Laboratory. The real-time CFTR quantitative PCR analysis was obtained on RNA extracted from cell lysates. Total RNA was extracted using TRIzol Reagent (Invitrogen), and the PureLink Micro-to-Midi total RNA purification system (Invitrogen). Exon-spanning primers specific for CFTR and GAPDH, were designed on the basis of published cDNA sequences. Real-time PCR was performed using the 7500 Real-Time PCR system (Applied Biosystems, Foster City, CA), and results were reported as fold change versus GAPDH expression.

Western Blotting

Endothelial cells were lysed and then fractionated using the CellLytic MEM Protein Extraction Kit (Sigma), to enrich for membrane proteins from hydrophobic fractions. Lysates were loaded in equal amounts (30 μg protein/lane) on SDS-PAGE followed by immunoblotting as previously described (14, 15). Membranes were incubated with CFTR-specific antibody (1:200; Upstate, Billerica, MA), followed by anti-mouse biotin-conjugated antibody, 1:10,000 diluted in TBST and a tertiary anti-biotin horseradish peroxidase–linked antibody, 1:10,000.

Apoptosis Assays

Apoptosis was induced in endothelial cells by treatment with staurosporine (0.6 μM, 6 h) or H_2O_2 (250–500 μM, 2–6 h) in serum-free culture media. Caspase-3 activity was measured in cell lysates using

a fluorescence-based assay (Promega) as previously described (16). Annexin and propidium iodide staining was used to identify apoptotic cells and exclude necrosis, using a fluorescence-based assay (R&D Systems, Minneapolis, MN), quantified by flow cytometry.

Lipid Extraction

Lipid extraction was performed by the Bligh and Dyer method by suspending cells in chloroform:methanol:water with a ratio of 0.5:1:0.4 (vol/vol/vol) in glass tubes. The lipid phase was separated by addition of chloroform and water (1:1) followed by centrifugation. The lower organic phase was saved and the total phospholipid content was determined by colorimetric phosphate quantification (17). This determination was used for normalization of ceramide and S1P measurements (15).

Ceramide and S1P Quantification

Analyses of the sphingolipids were performed via combined liquid chromatography-tandem mass spectrometry (LC/MS/MS). Instrumentation employed was an API4000 Q-trap hybrid triple quadrupole linear ion-trap mass spectrometer (Applied Biosystems) equipped with turboionspray ionization source and Agilent 1100 series liquid chromatograph as a front end (Agilent Technologies, Wilmington, DE).

The sphingolipids were ionized via electrospray ionization (ESI) with detection by multiple reaction monitoring (MRM). Analysis of the molecular species of sphingoid bases and ceramides employed positive ion ESI with MRM analysis with minor modification of published methods (18, 19) as previously described (20). C_{17}-analogs of ceramide and S1P were used as internal standards (15). The MRM transitions employed for detection of sphingoid bases were as follows: m/z 286 > 268 (C17-sphingosine, internal standard); m/z 300 > 282 (sphingosine); and m/z 302 > 284 (dihydrosphingosine). MRM transitions monitored for the elution of ceramide molecular species were as follows: m/z 510 > 264, C14:0-ceramide; m/z 538 > 264, C16:0-ceramide; m/z 540 > 284, C16:0-dihydroceramide; m/z 552 > 264, C17:0-ceramide (internal standard); m/z 564 > 264, C18:1-ceramide; m/z 566 > 284, C18:1-dihydroceramide; m/z 566 > 264, C18:0-ceramide; m/z 568 > 284, C18:0-dihydroceramide; m/z 594 > 264, C20:0-ceramide; m/z 650 > 264, C24:1-ceramide; m/z 652 > 284, C24:1-dihydroceramide; m/z 652 > 264, C24:0-ceramide; m/z 654 > 284, C24:0-dihydroceramide; m/z 680 > 264, C26:1-ceramide; m/z 682 > 264, C26:0-ceramide; m/z 708 > 264, C28:1-ceramide; m/z 710 > 264, C28:0-ceramide). S1P and DHS1P were quantified as *bis*-acetylated derivatives employing reverse-phase HPLC separation, negative ion ESI, and MRM analysis. Details of this approach are as previously described (21).

Enzymatic Activity Assays

Neutral and acid sphingomyelinase activities were measured in cell lysates using a fluorescence-based assay (Invitrogen) as previously described (22). RIPA buffer with proteinase inhibitors was used to obtain cell lysates, which were then further diluted in the appropriate acid or nonacid buffer per the assay protocol. Serine palmitoyltransferase activity was determined as previously described (22). In brief, cells were lysed in lysis buffer (10 mM HEPES [pH 7.5], 250 mM sucrose, 1 mM EDTA) plus protease inhibitor cocktail and sonicated on ice. Supernatants were collected and 100 μl added to an equal volume of 2× assay buffer (0.2M HEPES pH 8.3, 5 mM EDTA, 100μM pyridoxal phosphate, 10 mM DTT, 2 mM L-serine). Samples were incubated for 10 minutes at 37°C. The reaction was initiated by the addition of palmitoyl-CoA to a final concentration of 0.2 mM and 1.0μCi of [^{3}H] serine and incubated at 37°C for 7 minutes. Reactions were terminated by the addition of NH_4OH (3 ml, 0.5 N) and chloroform/methanol (2:1 vol/vol), 25 μg D-sphingosine, followed by NH_4OH (2 ml, 0.5 N). The lower organic phase was collected, dried under a stream of nitrogen, and resuspended in 1 ml scintillation fluid. CPMs were counted using a PE TopCount NXT scintillation counter.

Acidic/basic pH treatments were achieved by preparing media from basal EMB-2 using Tris-HCl (30 mM) and Hepes (40 mM) buffers, followed by pH adjustments to 6.5, 7.0, 7.4, 7.8, and 8.0 with HCl and/or NaOH (24). Media was then placed in a 37°C, 5% CO_2 incubator for 24 to 48 hours to allow equilibration with CO_2. The pH of the media was monitored before adding it to cells and at the completion of experiments.

Human lung tissue consisted of sections from fixed, paraffin-embedded explanted lung tissue from patients with chronic obstructive pulmonary disease (COPD) and from patients with CF (collected at the University of Pittsburgh). Normal lung tissue sections were generously provided by Dr. Rubin Tuder (Johns Hopkins University and the University of Colorado). The specimen collection and storage were approved by the Institutional Research Board from the University of Pittsburgh and the Johns Hopkins University.

Immunohistochemical staining for active caspase-3 was performed on paraffin-embedded lung sections according to the manufacturer's directions using the Vector antigen unmasking solution and the Vectastain Universal Elite ABC kit (Vector Laboratories, Burlingame, CA). Briefly, after blocking with 2% normal horse serum, an anti-active caspase-3 polyclonal antibody (Ab2302; Abcam, Cambridge, MA) at dilution of 1:25 was applied as the primary antibody for 2 hours. The antibody diluent (DAKO, Carpinteria, CA), without the primary antibody, was used as negative control. The sections were then incubated with horse "universal" anti-mouse/rabbit IgG (biotinylated antibody) for 30 minutes. After washing with TBST, a complex of avidin and biotinylated horseradish peroxidase was applied to the sections for 30 minutes. After washing with TBST, the sections were developed with Vector diaminobenzidine (DAB) substrate kit (Vector). A similar staining procedure was performed omitting the primary antibody and was used as negative control.

TUNEL and endothelial cell–specific marker immunostaining were performed by first processing paraffin-embedded lung sections for the detection of TUNEL-positive apoptotic cells using commercially available Fluorescein FragEL DNA Fragmentation Detection Kit (Calbiochem, Gibbstown, NJ), according to the manufacturer's guidelines. Then, the CD31 endothelial cell–specific marker was visualized using a primary goat polyclonal CD31 antibody (1:50 dilution; Santa Cruz Biotechnology, Santa Cruz, CA) and Texas Red–conjugated rabbit anti-goat IgG (1:200 dilution; Santa Cruz). Nuclei were counterstained with 4′,6-diamidino-2-phenylindole (DAPI).

Stained slides were coded, and an individual blinded to the identity of the slides captured representative images from each lung using a Nikon Microscope equipped with a Nikon camera. For quantification of the staining intensity, the images were then scored using a Metamorph (Molecular Devices, Sunnyvale, CA) macro developed by Dr. Rubin M. Tuder (University of Colorado).

Statistical Analysis

Statistical analysis was performed using SigmaStat 3.5. The differences between groups were compared using unpaired Student *t* test or ANOVA with Student-Newman-Keuls. Statistical significance was set at $P < 0.05$.

RESULTS

Expression of Functional CFTR in Lung Endothelial Cells

It has been previously reported that CFTR is expressed in human umbilical vein cells and human lung microvascular endothelial cells, where it functions as a chloride channel (2). Using routine PCR (Figure 1A) and Western blotting (not shown), we confirmed the expression of CFTR in primary lung microvascular endothelial cells. CFTR expression was also identified in primary bronchial arteries endothelial cells from sheep by routine RT-PCR (Figure 1A), followed by sequencing that demonstrated the ovine CFTR sequence (data not shown). Patch clamp analysis of the CFTR ion channel showed activation by 8-Br-cAMP and genistein as expected, and inhibition of the channel by the prototypical specific CFTR inhibitors, DPC and NPPB, but not by the non-CFTR chloride channel inhibitor DIDS (Figure 1B, *i–iii*). To investigate whether oxidative stress alone modifies the CFTR current in lung endothelial cells, currents were recorded during 400-millisecond step pulses to −100 mV and +100 mV from the holding potential of 0 mV. The current amplitudes were averaged over a 380-millisecond interval. Since our pipette solution contained low chloride concentration (12 mM), we considered that any inward currents represent mostly leak currents or other nonselective cation

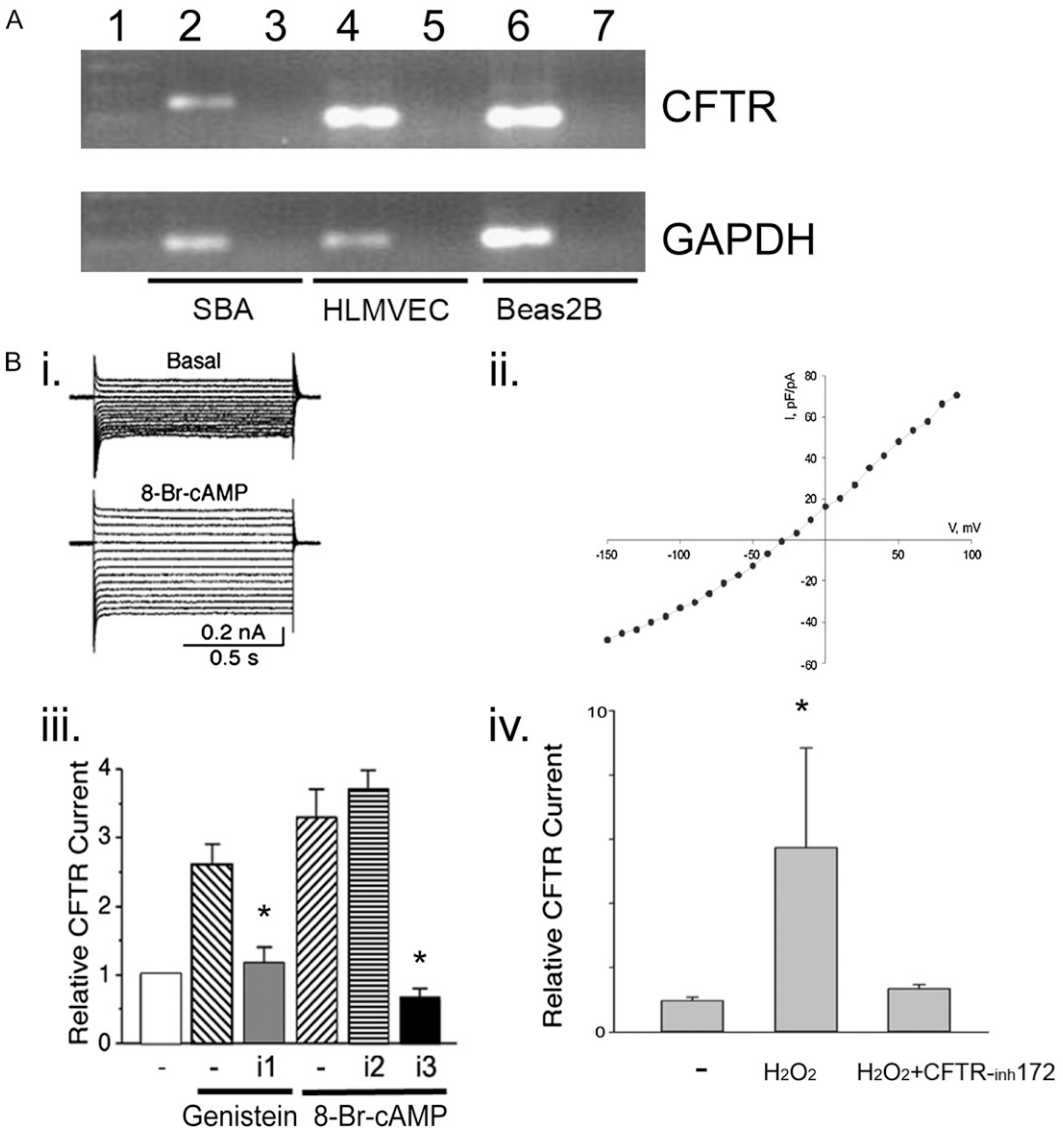

Figure 1. Cystic fibrosis (CF) transmembrane conductance regulator (CFTR) expression and ion channel function in lung endothelium. (*A*) CFTR RNA expression in sheep bronchial artery cells (SBA), human lung microvascular endothelial cells (HLMVEC), and BEAS-2B (bronchial epithelial cells, as control) was detected by routine RT-PCR. Size markers were loaded in *lane 1*; samples without reverse transcription (no RT, controls) were loaded into *lanes 3*, *5*, and *7*. (*B*) CFTR current recording by whole cell patch clamp analysis in HLMVEC. (*i*) Traces of Cl^- currents recorded before (*top*) and after (*bottom*) application of 8-Br-cAMP (100 μM). Currents were evoked by voltage steps ranging from −100 mV to 50 mV from a holding potential of 0 mV. (*ii*) I–V curve of CFTR currents (I expressed as current density). (*iii*) Effects of CFTR channel activator and blocker on Cl^- currents. Mean CFTR currents recorded in the presence of CFTR activators (genistein, 100 μM or 8-Br-cAMP, 100 μM) and specific CFTR inhibitors DPC (i_1, 200 μM) or NPPB (i_3, 200 μM) or non-CFTR Cl^- channel inhibitor DIDS (i_2, 200 μM). The currents were normalized to those recorded before application of the drugs (evoked at 50 mV) and reported as relative currents (mean ± SD; $*P < 0.05$). (*iv*) Relative CFTR currents recorded in the absence (−) or presence of H_2O_2 and the effect of $CFTR_{inh}172$ (100 μM) (mean ± SEM; $*P < 0.05$).

conductance. The outward chloride current component was isolated by subtracting the absolute value of the inward current from the total outward current. The resulting outward currents, expressed relative to the cell capacitance, were significantly larger in the H_2O_2-treated cells and were reduced in cells treated with both H_2O_2 and the CFTR inhibitor $CFTR_{inh}$-172 (Figure 1B, *iv*). These results suggested that CFTR is expressed on both pulmonary and bronchial artery endothelial cells, where it functions as a chloride channel that may be activated by oxidative stress. Next, we set out to determine the role of CFTR function in endothelial cell viability and death.

Effect of CFTR Inhibitors on Endothelial Cell Viability

CFTR function was modulated using pharmacologic inhibitors DPC, NPPB, and $CFTR_{inh}$-172 at concentrations that demonstrated effective CFTR inhibition by patch clamp analysis. The effect of these inhibitors, the non-CFTR chloride channel inhibitor DIDS, or the CFTR activator genistein on the baseline endothelial cell viability was studied using the LDH release assay, having their vehicle (ethanol or DMSO) as controls. The effective concentration of the inhibitor that effectively blocked the CFTR chloride current in the patch clamp analyses was 200 μM for DPC and NPPB. At these concentrations, the CFTR inhibitors failed to induce endothelial cell death at 30 minutes and at 16 hours after treatment, with the exception of NPPB, which increased LDH release at 16 hours (Figure E1 in the online supplement, and data not shown). Based on these results, nontoxic concentrations of inhibitors were used in subsequent experiments that assessed their effect on endothelial cell apoptosis.

Pulmonary endothelial cell apoptosis was studied in response to staurosporine, a general protein kinase inhibitor, or to H_2O_2, an inducer of oxidative stress. Mouse lung endothelial cells pretreated with the specific CFTR inhibitors DPC or NPPB demonstrated significant attenuation of staurosporine-induced apoptosis, as measured by Annexin V/propidium iodide staining and flow cytometry (Figure 2A) or caspase-3 activity assay (data

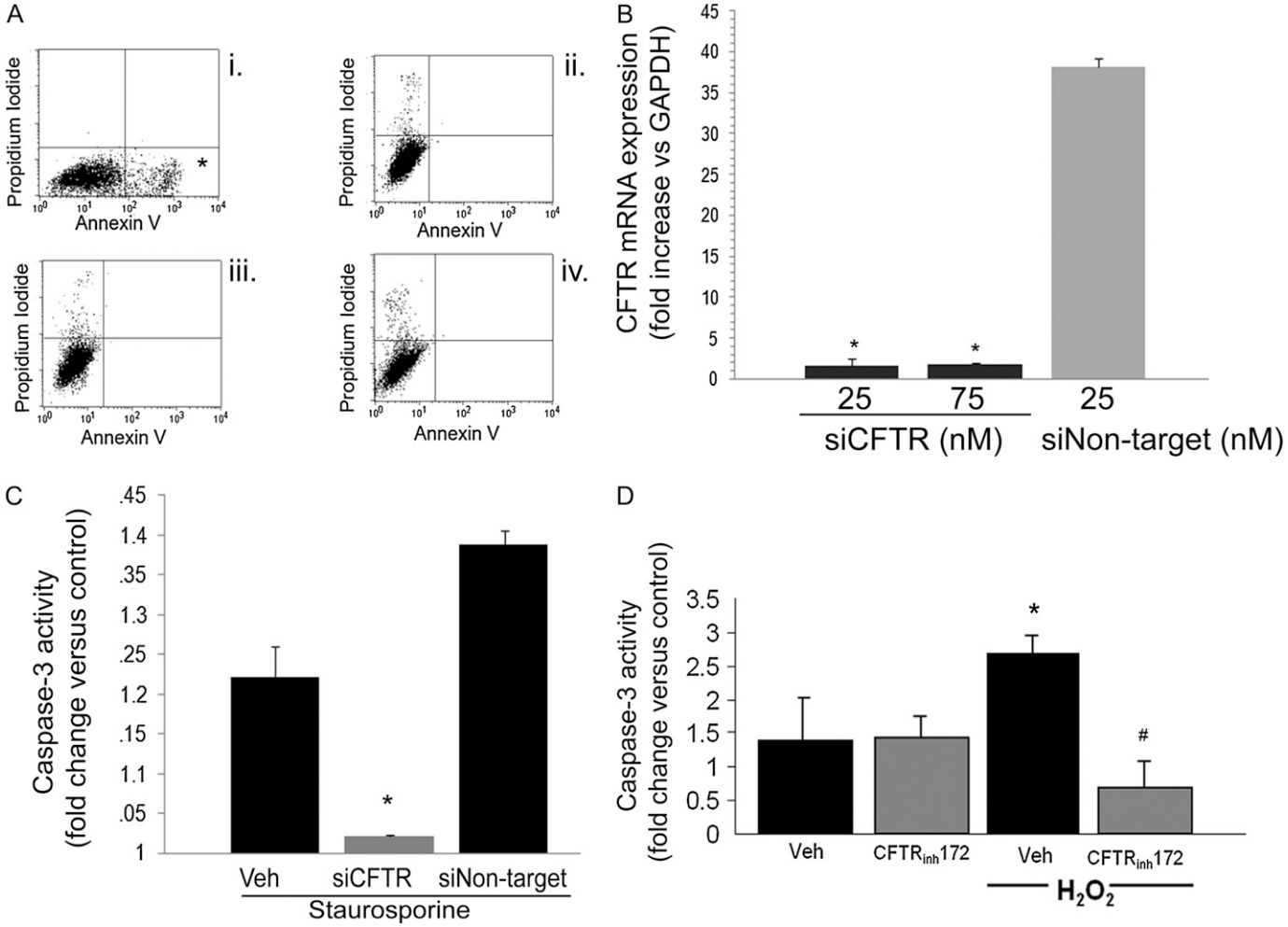

Figure 2. Effect of CFTR inhibitors on stress-induced lung endothelial cell apoptosis. (*A*) Flow cytometry of mouse lung endothelial cells stained with Annexin V and propidium iodide and treated with (*i*) staurosporine (0.6 μM, 6 h), (*ii*) vehicle, and staurosporine with (*iii*) DPC (200 μM) or (*iv*) NPPB (200 μM) pretreatments. Note marked increase in apoptotic cells in the *right lower quadrant* (*asterisk*) in the staurosporine-treated cells and the profound inhibition of apoptosis in the CFTR-inhibited cells. (*B*) CFTR mRNA expression (relative to GAPDH) measured in endothelial cells by real-time PCR after transient transfection with siRNA targeting CFTR (siCFTR) at the indicated concentrations or with nontarget siRNA ($n = 2$; mean ± SD; $^*P < 0.05$ versus nontarget siRNA). (*C*) Caspase-3 activity in primary human lung microvascular endothelial cells treated with staurosporine (0.6 μM, 6 h) with or without siCFTR (25 nM) or nontarget siRNA (25 nM). Caspase-3 activity was measured in cell lysates as U/μg protein/minute and reported as fold increase versus each respective untreated control ($n = 3$; mean ± SEM; $^*P < 0.05$ versus nontransfected cells and versus nontarget siRNA-transfected cells). (*D*) Caspase-3 activity in primary human lung microvascular endothelial cells treated with H_2O_2 (250 μM, 6 h) in the presence of the CFTR inhibitor $CFTR_{inh}$-172 (20 μM). Caspase-3 activity was measured in cell lysates and expressed as U/μg protein/min and then reported as fold increase versus control, untreated cells ($n = 3$; mean ± SEM; $^*P < 0.05$ versus control; $^{\#}P < 0.05$ versus H_2O_2 treatment).

not shown). Knockdown of CFTR via transient transfection of endothelial cells with a specific siRNA (25–75 nM for 72 h) significantly reduced CFTR RNA expression as measured by real-time PCR compared with transfection with a nontarget siRNA (Figure 2B). CFTR knockdown (25 nM for 72 h) significantly inhibited staurosporine-induced apoptosis in lung endothelial cells, measured by caspase-3 activity assay (cells had a nonstatistical significant increase of 2% [1.02-fold] in caspase-3 activity versus control) (Figure 2B). In contrast, nontarget siRNA treatment failed to reduce staurosporine-induced apoptosis (1.4-fold increase in caspase-3 activity versus control) compared with cells that did not receive siRNA and underwent staurosporine-induced apoptosis (which had approximately a 1.2-fold increase in caspase-3 activity versus control; Figure 2C). A similar effect was obtained after pretreatment with the highly specific CFTR inhibitor $CFTR_{inh}$-172, which significantly attenuated H_2O_2-induced primary human pulmonary microvascular endothelial cell apoptosis measured by caspase-3 activity assay (Figure 2D). The nonspecific chloride channel DIDS also inhibited H_2O_2-induced apoptosis in human and mouse pulmonary endothelial cells (data not shown), implying that other chloride ion channel flows may also facilitate apoptosis induced by oxidative stress in these cells.

Mechanisms of CFTR Involvement in Endothelial Cell Apoptosis

Ceramide is a second messenger in endothelial cell apoptosis signaling in response to multiple agonists, including oxidative stress. Treatment of human microvascular endothelial cells with H_2O_2 significantly increased intracellular ceramide levels (by ~20%), as quantified by tandem mass spectrometry (Figure 3A). Pretreatment of these cells with the CFTR inhibitor $CFTR_{inh}$-172 attenuated H_2O_2-induced ceramide up-regulation (Figure 3A). Interestingly, the inhibition of CFTR did not alter either in-

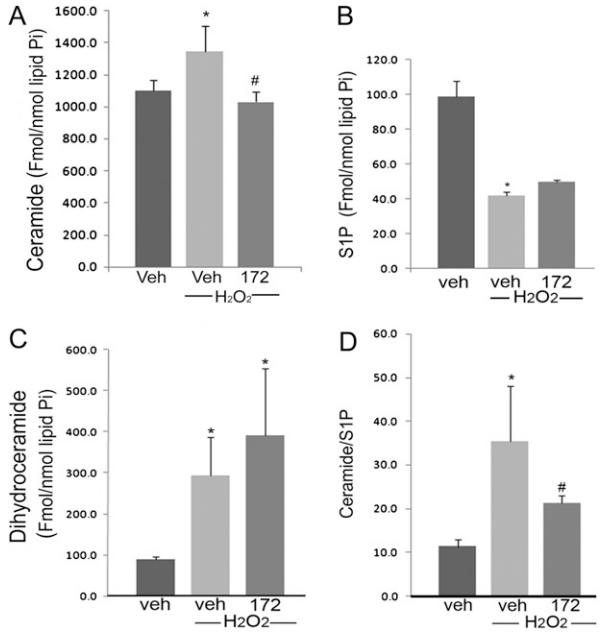

Figure 3. Effect of CFTR inhibitors on intracellular sphingolipid levels in lung endothelial cells. (*A–C*) Ceramide, S1P, and dihydroceramide levels were measured by tandem mass spectrometry in primary human lung microvascular endothelial cells treated with H_2O_2 (250 μM, 6 h) in the presence of the CFTR inhibitor $CFTR_{inh}$-172 (20 μM). Sphingolipid levels were normalized by intracellular phospholipids (inorganic phosphorus content, Pi) and plotted as mean ± SEM ($n = 3$; $^*P < 0.05$ versus control; $^{\#}P < 0.05$ versus H_2O_2). (*D*) The ratio of ceramide/S1P in lung endothelial cells, an indicator of pro-apoptotic/anti-apoptotic intracellular balance, was calculated from the values measured in *A* and *B* (mean ± SEM; $n = 3$; $^*P < 0.05$ versus control; $^{\#}P < 0.05$ versus H_2O_2 treatment).

tracellular levels of S1P (which were decreased by H_2O_2) (Figure 3B), or the dihydroceramide levels (Figure 3C), precursors of ceramide in the *de novo* pathway of ceramide synthesis (which were increased by H_2O_2). Overall, CFTR inhibition significantly decreased the ceramide:S1P ratio in endothelial cells (Figure 3D), suggesting that the anti-apoptotic effects of CFTR inhibition were due to a decrease in the net pro-apoptotic levels of intracellular sphingolipids.

To investigate whether the decrease in intracellular ceramide levels was required by the CFTR inhibitor to inhibit apoptosis, we supplemented lung endothelial cells with sphingomyelinase. Sphingomyelinase catalyzes the breakdown of sphingomyelin from the membranes to generate ceramide. Treatment of human lung microvascular endothelial cells with a low concentration of sphingomyelinase, which by itself is not sufficient to cause apoptosis, effectively reversed the $CFTR_{inh}$-172 anti-apoptotic action against H_2O_2 (Figure 4A). These results suggested the CFTR inhibition results in an apoptosis-resistant cellular state due to an inability to up-regulate ceramides in response to stress.

Decreases in cytosolic pH precede cytochrome c release and caspase activation (24). Intracellular acidification is also necessary for the activation of enzymes, such as acid sphingomyelinase and ceramidase, which typically cause increases and decreases in intracellular ceramide levels, respectively. Previous work showed that CFTR-deficient epithelial cells are unable to acidify their cytoplasm secondary to lack of bicarbonate outflow (8). We therefore investigated next the role of pH in the anti-apoptotic effect of the CFTR inhibitors. Human endothelial

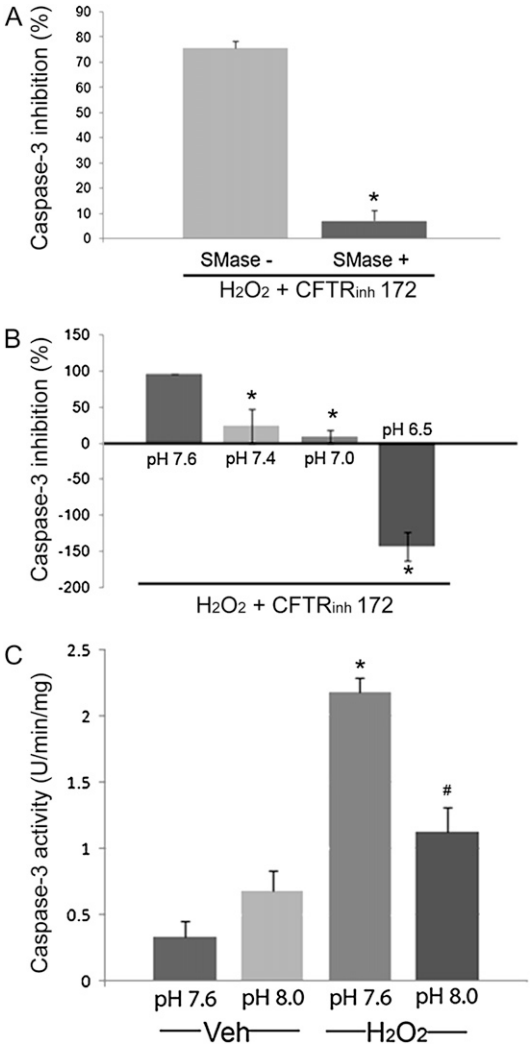

Figure 4. Modulation of apoptotic susceptibility to H_2O_2 of CFTR-inhibited endothelial cells. (*A*) Inhibitory potency of $CFTR_{inh}$-172 on the apoptosis induced by H_2O_2-treated human lung microvascular endothelial cells was measured by caspase-3 activity. Results were expressed as % inhibition of maximum H_2O_2-induced caspase-3 activation (mean ± SEM; $n = 6$; $^*P < 0.01$). Cells were pre-treated with $CFTR_{inh}$-172 (20 μM) before H_2O_2 (250 μM, 6 h) with or without supplementation with sphingomyelinase (0.3 U/ml). Note that in the presence of this low concentration of sphingomyelinase, $CFTR_{inh}$-172 lost its ability to inhibit H_2O_2-induced apoptosis. (*B*) Inhibitory potency of $CFTR_{inh}$-172 on H_2O_2-induced endothelial cells apoptosis was expressed as % inhibition of maximum H_2O_2-induced caspase-3 activation (mean ± SEM; $n = 3$; $^*P < 0.05$). Cells were pre-treated with $CFTR_{inh}$-172 (20 μM) before H_2O_2 (250 μM, 6 h) at various pH of the culture medium, as indicated. Note a loss of apoptosis inhibitory capacity of $CFTR_{inh}$-172 with decreasing the cell media pH (acidification) compared with the pH of the usual culture media (pH 7.6). (*C*) Apoptosis measured by caspase-3 activity in human lung microvascular endothelial cells after treatment with H_2O_2 (250 μM, 6 h) at various pH of the culture medium, as indicated (mean ± SD; $n = 3$; $^*P < 0.01$ versus Veh at pH 7.6; $^{\#}P < 0.01$ versus H_2O_2 at pH 7.6). Note inhibition of H_2O_2 -induced endothelial cells apoptosis when cells are at a higher pH (alkalinization) compared with the pH of the usual culture conditions (pH 7.6).

cells treated with $CFTR_{inh}$-172 in an acidified media (pH 6.5 and 7.0, rather than a pH of 7.6 measured in regular growth media) showed increased susceptibility to H_2O_2-induced apoptosis, inversely related with the intracellular pH (Figure 4B). Conversely,

the alkalinization of endothelial cells (exposure to media with pH 7.8 and 8.0) alone rendered them more resistant to H_2O_2-induced apoptosis, recapitulating the phenotype induced by CFTR inhibition (Figure 4C).

To investigate whether the effect of CFTR inhibitor on the intracellular pH is linked to its effect on ceramide signaling, we measured the activity of key enzymes involved in controlling ceramide levels under varying pH conditions. In usual culture conditions, H_2O_2 treatment significantly increased the activity of serine palmitoyl transferase (SPT, Figure 5A), the first step in the *de novo* ceramide pathway, and had only a modest activation (not reaching statistical significance) effect on the acid sphingomyelinase (Figure 5B), but not neutral sphingomyelinase (not shown) activity. The activator effect of H_2O_2 on SPT and acid sphingomyelinase was significantly blocked by the $CFTR_{inh}$-172 (Figures 5A and 5B). These results indicate that the *de novo* pathway is the major contributor to the increased ceramide:S1P ratio after H_2O_2 treatment in lung endothelium, and importantly, that this increase is attenuated by CFTR inhibition. Under acidic (pH 6.8) culture conditions, endothelial cells treated with H_2O_2 failed to activate SPT (Figure 5C), whereas they enhanced the acid sphingomyelinase activity both at baseline (absolute activity almost doubled compared with the cells in usual baseline conditions shown in Figure 3B) and after H_2O_2 treatment (Figure 5D). Interestingly, the significant inhibitory effect of $CFTR_{inh}$-172 on the H_2O_2-induced acid sphingomyelinase activation persisted even in acidic conditions (Figure 5D). These results suggested that the pathway of restoration of CFTR-inhibited lung endothelial apoptosis by the acidic pH may be SPT and acid sphingomyelinase independent.

Levels of Endothelial Cell Apoptosis in Human Lung from Patients with CF

To determine the relevance of impaired stress-induced apoptosis in CFTR-inhibited human endothelial cells in culture conditions, we measured levels of apoptosis in lungs of patients with CF. Apoptosis was determined in lung tissue from patients with CF or from those suffering from the chronic lung disease COPD (by TUNEL and active caspase-3 immunohistochemistry) and from individuals without lung disease (active caspase-3 immunohistochemistry). To determine the levels of apoptosis specifically in lung endothelial cells *in vivo*, lungs were co-stained for TUNEL and CD31, an endothelial cell–specific marker. Compared with the lungs from patients with COPD (a chronic lung disease characterized by airway inflammation, known to exhibit elevated apoptosis of alveolar cells [25]), the CF lungs had sparse TUNEL-positive lung cells that seldom co-localized with endothelial cells (Figure 6A). To confirm that the TUNEL-positive cells were indicative of apoptosis, we performed immunohistochemistry for active caspase-3. Similarly, CF lung tissue showed markedly lower active caspase-3 immunostaining compared with COPD (Figure 6B). When measured by image analysis software, the intensity of the active caspase-3 in the CF lung parenchyma was as low as in nondiseased lung samples, and significantly diminished compared with the COPD alveolar parenchyma (Figure 6B, *panel f*). In both CF and COPD lung tissue sections examined, there was minimal apoptosis in the large airways epithelium (Figure 6A, *panels c* and *f*).

DISCUSSION

Our studies indicate that one of the roles of CFTR in lung endothelium is to facilitate pro-apoptotic signaling in response to stresses such as oxidative stress. Inhibition of CFTR in endothelial cells was associated with an inability to up-regulate ceramides in response to oxidative stress and was linked to the inability of CFTR-inhibited cells to acidify the intracellular milieu, a step required for optimal activity of several pro-apoptotic pathways. Restoration of either ceramide levels or of an acidic pH was sufficient alone to overcome the CFTR-inhibitors' anti-apoptotic

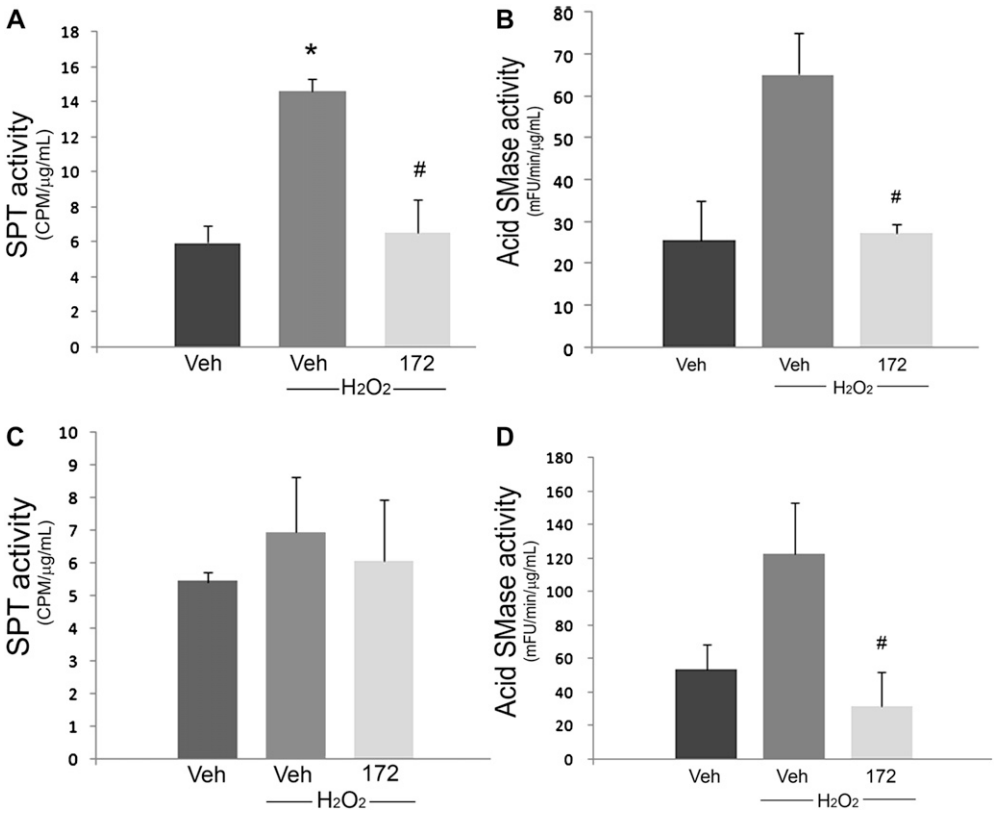

Figure 5. Modulated enzyme activity in CFTR-inhibited endothelial cells in acidic and neutral conditions. (*A*) Serine palmitoyl transferase and (*B*) acid sphingomyelinase activities measured in human lung microvascular endothelial cells after pretreatment with $CFTR_{inh}$-172 (20 μM) and treatment with H_2O_2 (250 μM, 1 h) in usual culture conditions (pH 7.6). (*C*) Serine palmitoyl transferase and (*D*) acid sphingomyelinase activities measured in human lung microvascular endothelial cells after pretreatment with $CFTR_{inh}$-172 (20 μM) and H_2O_2 (250 μM, 1 h) at pH 6.8 (mean ± SD; $n = 2$ for *A* and *C*, $n = 3$ for *B* and *D*; $^*P < 0.05$ versus Veh; $^{\#}P < 0.05$ versus H_2O_2).

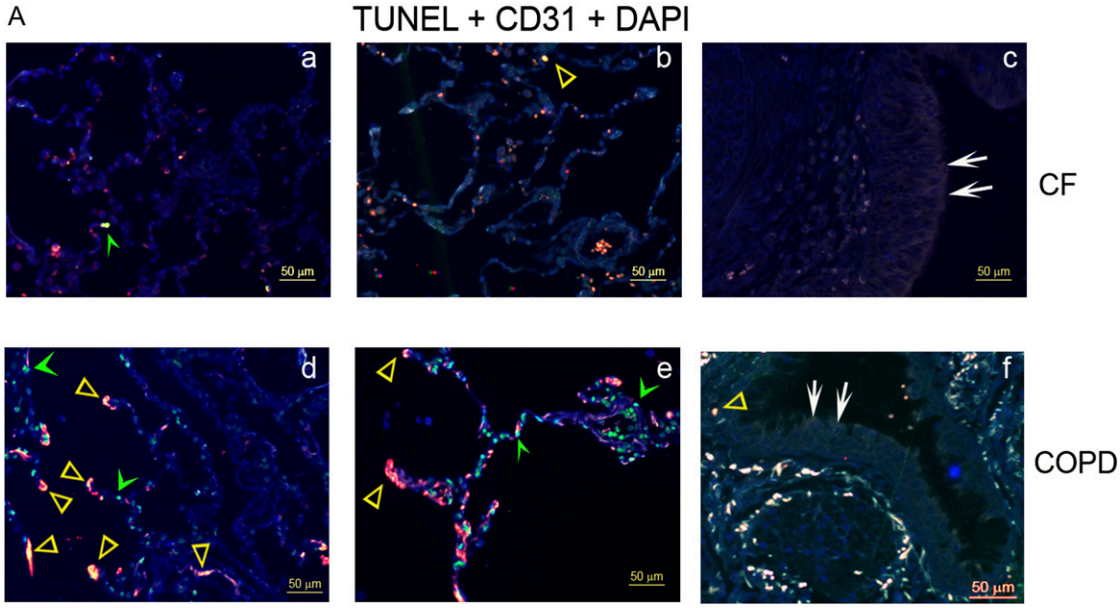

Figure 6. Apoptosis levels in human CF lungs. (*A*) Representative human lung sections from patients with (*a–c*) CF or (*d–f*) chronic obstructive pulmonary disease (COPD), co-stained for apoptosis (TUNEL; *green*; *green arrowhead*), endothelial cells (CD-31; *red*), and nuclei (DAPI; *blue*). Note the relative paucity of apoptotic endothelial cells (*yellow*; *yellow open arrowhead*) in the CF lungs compared with COPD lungs. There was little TUNEL staining in the large airway epithelium (*white arrows*) in both CF and COPD (*c*, *f*). (*B*) Representative micrographs of active caspase-3 immunostaining (*brown staining*, *arrows*) of fixed samples from (*a*, *b*) CF, (*c*, *d*) COPD, and (*e*) nondiseased human lungs (*arrowheads* pointing to carbon particles). (*f*) The positive staining was quantified by image analysis software and expressed as density units per high-power field of lung (mean ± SEM; 3–9 random fields per sample; $n = 4$ CF and COPD samples each from a different individual; $n = 3$ nondiseased lungs each from a different individual; $^*P < 0.01$).

effect. The inhibition of oxidative stress–induced lung endothelial cell apoptosis by the CFTR inhibition was paralleled by a decrease in apoptosis in general, and endothelial cell apoptosis in particular, in CF lungs.

Although the presence of CFTR in cells other than epithelium is now well documented (2, 26–28), its role in these cellular compartments, particularly in the endothelium, is not well known. Our work contributes to the understanding of the role of CFTR in lung endothelial cell viability. Previous studies in lung epithelial cells and CF mouse lung and gastrointestinal disease models have generated conflicting results for the role of CFTR in apoptosis. An anti-apoptotic role for CFTR in airway epithelial cells was noted in the lungs of aged CFTR-null mice, which exhibited increased apoptosis due to excessive accumulation of ceramide (9). Similar to our results, an apoptosis facilitator role for CFTR was noted in lung epithelial cells under stress from pseudomonal infection (7) and in a mouse model of CF-associated gastrointestinal disease (29). These results suggest that the role of CFTR in apoptosis may be cell type and stimulus dependent and may differ at different ages. For example, defective CFTR may lead to altered regulation of sphingolipid metabolism, leading to abnormally high levels of ceramide in cells with genetic long-standing CFTR deficiency (9), and additionally impair ceramide up-regulation under stress, as demonstrated by the current work.

The interrelation of CFTR and sphingolipids is complex. CFTR is inserted in sphingolipid-rich membrane domains, which play a role in both apoptotic signaling (30) and the internalization of *Pseudomonas aeruginosa* (31), events of relevance to CF pathogenesis. While CFTR function itself may be modulated by ceramides (32) through its function as an ATP-binding cassette, CFTR has also been implicated in the transport of sphingolipids across the plasma membrane, in particular the transport of S1P into cells (13). Our data indicated that ceramide levels are decreased in CFTR-inhibited cells undergoing oxidative stress, whereas S1P levels were not affected, indicating the driving factor toward cell survival in CFTR-inhibited cells was through impaired ceramide production, rather than S1P availability. These results are in agreement with the report by Guilbault and coworkers that showed decreased circulating levels of specific ceramide species in the plasma of individuals with CF and decreased lung levels of ceramide in mice deficient of CFTR (33). These findings reveal the importance of using mass spectrometric documentation of ceramide content to accurately discern between ceramides and dihydroceramides levels. Although previously thought to be biologically inactive, there is accumulating evidence that dihydroceramides may exert independent biological effects, including opposing ceramide functions (34). Although it remains unclear what role dihydroceramides play in the CFTR-inhibited endothelium, their accumulation in the context of decreased ceramide levels was associated with inhibition of apoptosis. The mechanism by which ceramide levels were decreased while dihydroceramide levels were increased by the CFTR inhibitors remains unclear, although it may be related to the sum of actions on the activity of enzymes regulating ceramide and dihydroceramide levels. As noted here in lung endothelial cells, H_2O_2 has been shown to increase SPT activity in other cell types (35). Both the acid sphingomyelinase and SPT activation were inhibited by the CFTR inhibitor. The lack of S1P and dihydro-S1P accumulation implies that sphingosine kinase is not activated. In this context, the increased dihydroceramide levels may be explained by decreased N-acyl-sphinganine dehydrogenase activity, which would block the conversion of dihydroceramide to ceramide (20).

Our data showed that acidification restores the susceptibility to stress-induced apoptosis in CFTR-inhibited lung endothelial cells, implicating pH-dependent processes in the impairment of apoptosis. One of the mechanisms implicated in the anti-apoptotic effects of CFTR inhibition in other cell types has been the lack of chloride and bicarbonate flow through an inhibited CFTR, which may impair the cell's ability to acidify and activate endonucleases required for apoptosis (8). Other enzymes implicated in apoptosis are pH regulated, including enzymes participating in the ceramide metabolism. To this end, Teichgräber and colleagues discovered the role of pH regulation of the reverse ceramidase activity, causing increased ceramides levels in the CFTR-null epithelial cells (9). However,

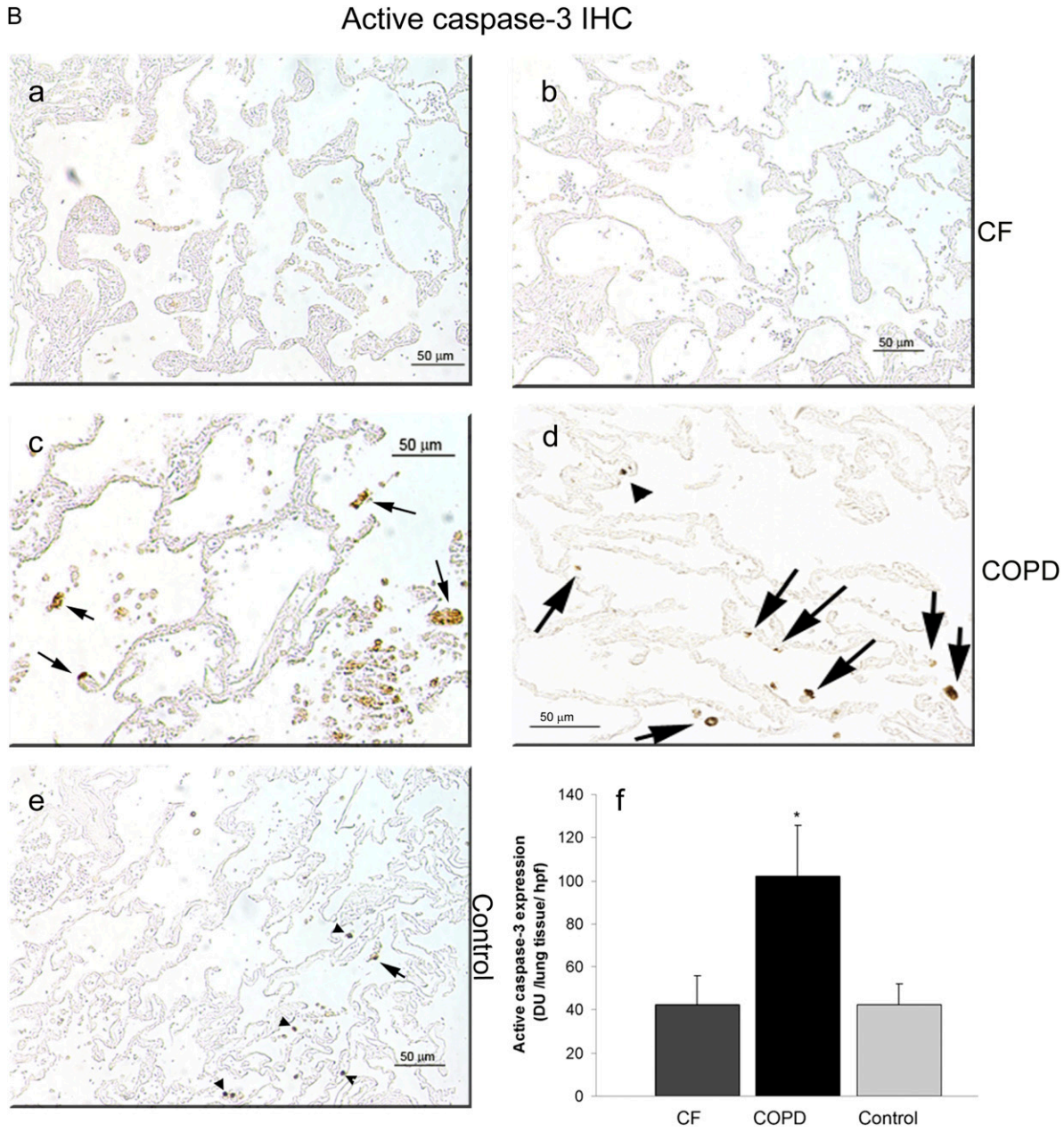

Figure 6. (*continued*).

our data suggested that in the context of decreased ceramide levels in CFTR-inhibited lung endothelial cells, lowering the intracellular pH, while restoring the susceptibility to apoptosis, did not abolish the effect of the CFTR inhibitor on the acid sphingomyelinase. It is therefore conceivable that the lack of CFTR acidification impairs apoptosis via pathways independent of acid sphingomyelinase. Other mechanisms by which CFTR facilitates oxidative stress–induced apoptosis may be present, including those shared by other chloride channels (as suggested by the anti-apoptotic action of the anion channel inhibitor DIDS). These mechanisms may include cell volume regulation (36, 37) and promoting $O_2^{\cdot -}$ flux across the endothelial cell membrane leading to intracellular Ca^{2+} release and apoptosis (38).

The relevance of a requirement for functional CFTR in stress-induced endothelial cell apoptosis is not yet known. Endothelial cell apoptosis has been invoked as a potential pathogenic mechanism in acute events such as sepsis and acute lung injury (39, 40) and in chronic diseases such as COPD-emphysema (25). Unlike our findings in the CF lung and CFTR-inhibited endothelial cells, emphysematous human lungs have increased apoptosis and increased ceramide levels (15, 41). It is unclear whether patients with CF have a lower incidence of acute lung injury or emphysema. One speculation awaiting further experimental studies is that an activated endothelium (for example, in bronchial arteries accompanying large airways) unable to undergo apoptosis could lead to aberrant angiogenesis or fuel local production of inflammatory cytokines and promote leukocyte migration, thus contributing to a heightened inflammatory state in the CF airway.

In conclusion, we have shown that CFTR function plays an essential role in stress-induced apoptosis of the lung endothelium. The CFTR inhibition had a pH-dependent anti-apoptotic effect involving decreases of intracellular ceramides in lung endothelial cells. This mechanism may be relevant to vascular

biology in general and to future studies aimed at understanding how lung vascular function contributes to the development of chronic inflammatory changes in CF.

Conflict of Interest Statement: None of the authors has a financial relationship with a commercial entity that has an interest in the subject of this manuscript.

Acknowledgments: The authors thank Dr. Aruna Sannuti (Adult CF Center Director, Indiana University) for helpful discussions regarding the interpretation of our data in light of relevance to clinical CF.

References

1. Ratjen F, Doring G. Cystic fibrosis. *Lancet* 2003;361:681–689.
2. Tousson A, Van Tine BA, Naren AP, Shaw GM, Schwiebert LM. Characterization of cftr expression and chloride channel activity in human endothelia. *Am J Physiol* 1998;275:C1555–C1564.
3. Robert R, Thoreau V, Norez C, Cantereau A, Kitzis A, Mettey Y, Rogier C, Becq F. Regulation of the cystic fibrosis transmembrane conductance regulator channel by beta-adrenergic agonists and vasoactive intestinal peptide in rat smooth muscle cells and its role in vasorelaxation. *J Biol Chem* 2004;279:21160–21168.
4. Noe JDP, Petrusca D, Smith P, Xu Z, Petrache I. The role of cftr in stress-induced apoptosis of human lung endothelial cells. *Am J Respir Cell Mol Biol* 2007;175:A931.
5. Savill J. Apoptosis in resolution of inflammation. *Kidney Blood Press Res* 2000;23:173–174.
6. Hotchkiss RS, Dunne WM, Swanson PE, Davis CG, Tinsley KW, Chang KC, Buchman TG, Karl IE. Role of apoptosis in *Pseudomonas aeruginosa* pneumonia. *Science* 2001;294:1783.
7. Cannon CL, Kowalski MP, Stopak KS, Pier GB. *Pseudomonas aeruginosa*–induced apoptosis is defective in respiratory epithelial cells expressing mutant cystic fibrosis transmembrane conductance regulator. *Am J Respir Cell Mol Biol* 2003;29:188–197.
8. Gottlieb RA, Dosanjh A. Mutant cystic fibrosis transmembrane conductance regulator inhibits acidification and apoptosis in c127 cells: possible relevance to cystic fibrosis. *Proc Natl Acad Sci USA* 1996;93:3587–3591.
9. Teichgräber V, Ulrich M, Endlich N, Riethmuller J, Wilker B, De Oliveira-Munding CC, van Heeckeren AM, Barr ML, von Kurthy G, Schmid KW, *et al.* Ceramide accumulation mediates inflammation, cell death and infection susceptibility in cystic fibrosis. *Nat Med* 2008; 14:382–391.
10. Castillo SS, Levy M, Thaikoottathil JV, Goldkorn T. Reactive nitrogen and oxygen species activate different sphingomyelinases to induce apoptosis in airway epithelial cells. *Exp Cell Res* 2007;313:2680–2686.
11. Goldkorn T, Balaban N, Shannon M, Chea V, Matsukuma K, Gilchrist D, Wang H, Chan C. H2O2 acts on cellular membranes to generate ceramide signaling and initiate apoptosis in tracheobronchial epithelial cells. *J Cell Sci* 1998;111:3209–3220.
12. Medler TR, Petrusca DN, Lee PJ, Hubbard WC, Berdyshev EV, Skirball J, Kamocki K, Schuchman E, Tuder RM, Petrache I. Apoptotic sphingolipid signaling by ceramides in lung endothelial cells. *Am J Respir Cell Mol Biol* 2008;38:639–646.
13. Boujaoude LC, Bradshaw-Wilder C, Mao C, Cohn J, Ogretmen B, Hannun YA, Obeid LM. Cystic fibrosis transmembrane regulator regulates uptake of sphingoid base phosphates and lysophosphatidic acid: modulation of cellular activity of sphingosine 1-phosphate. *J Biol Chem* 2001;276:35258–35264.
14. Petrache I, Fijalkowska I, Zhen L, Medler TR, Brown E, Cruz P, Choe KH, Taraseviciene-Stewart L, Scerbavicius R, Shapiro L, *et al.* A novel anti-apoptotic role for alpha-1 antitrypsin in the prevention of pulmonary emphysema. *Am J Respir Crit Care Med* 2006;173:1222–1228.
15. Petrache I, Natarajan V, Zhen L, Medler TR, Richter AT, Cho C, Hubbard WC, Berdyshev EV, Tuder RM. Ceramide upregulation causes pulmonary cell apoptosis and emphysema-like disease in mice. *Nat Med* 2005;11:491–498.
16. Petrache I, Fijalkowska I, Medler TR, Skirball J, Cruz P, Zhen L, Petrache HI, Flotte TR, Tuder RM. {alpha}-1 antitrypsin inhibits caspase-3 activity, preventing lung endothelial cell apoptosis. *Am J Pathol* 2006;169:1155–1166.
17. Vaskovsky VE, Kostetsky EY, Vasendin IM. A universal reagent for phospholipid analysis. *J Chromatogr* 1975;114:129–141.
18. Murphy RC, Fiedler J, Hevko J. Analysis of nonvolatile lipids by mass spectrometry. *Chem Rev* 2001;101:479–526.
19. Merrill AH, Caligan TB, Wang E, Peters K, Ou J. Analysis of sphingoid bases and sphingoid base 1-phosphates by high-performance liquid chromatography. *Methods Enzymol* 2000;312:3–9.
20. Berdyshev EV, Gorshkova IA, Usatyuk P, Zhao Y, Saatian B, Hubbard W, Natarajan V. De novo biosynthesis of dihydrosphingosine-1-phosphate by sphingosine kinase 1 in mammalian cells. *Cell Signal* 2006;18:1779–1792.
21. Berdyshev EV, Gorshkova IA, Garcia JG, Natarajan V, Hubbard WC. Quantitative analysis of sphingoid base-1-phosphates as bisacetylated derivatives by liquid chromatography-tandem mass spectrometry. *Anal Biochem* 2005;339:129–136.
22. Medler TR, Petrusca DN, Lee PJ, Hubbard WC, Berdyshev EV, Skirball J, Kamocki K, Schuchman E, Tuder RM, Petrache I. Apoptotic sphingolipid signaling by ceramides in lung endothelial cells. *Am J Respir Cell Mol Biol* 2008;38:639–646.
23. Wesson DE, Simoni J, Green DF. Reduced extracellular ph increases endothelin-1 secretion by human renal microvascular endothelial cells. *J Clin Invest* 1998;101:578–583.
24. Segal MS, Beem E. Effect of pH, ionic charge, and osmolality on cytochrome c-mediated caspase-3 activity. *Am J Physiol Cell Physiol* 2001;281:C1196–C1204.
25. Kasahara Y, Tuder RM, Cool CD, Lynch DA, Flores SC, Voelkel NF. Endothelial cell death and decreased expression of vascular endothelial growth factor and vascular endothelial growth factor receptor 2 in emphysema. *Am J Respir Crit Care Med* 2001;163:737–744.
26. Robert R, Savineau JP, Norez C, Becq F, Guibert C. Expression and function of cystic fibrosis transmembrane conductance regulator in rat intrapulmonary arteries. *Eur Respir J* 2007;30:857–864.
27. Sun XC, Bonanno JA. Expression, localization, and functional evaluation of cftr in bovine corneal endothelial cells. *Am J Physiol Cell Physiol* 2002;282:C673–C683.
28. Vandebrouck C, Melin P, Norez C, Robert R, Guibert C, Mettey Y, Becq F. Evidence that cftr is expressed in rat tracheal smooth muscle cells and contributes to bronchodilation. *Respir Res* 2006;7:113.
29. Dimagno MJ, Lee SH, Hao Y, Zhou SY, McKenna BJ, Owyang C. A proinflammatory, antiapoptotic phenotype underlies the susceptibility to acute pancreatitis in cystic fibrosis transmembrane regulator (−/−) mice. *Gastroenterology* 2005;129:665–681.
30. Szabo I, Adams C, Gulbins E. Ion channels and membrane rafts in apoptosis. *Pflugers Arch* 2004;448:304–312.
31. Grassme H, Jendrossek V, Riehle A, von Kurthy G, Berger J, Schwarz H, Weller M, Kolesnick R, Gulbins E. Host defense against *Pseudomonas aeruginosa* requires ceramide-rich membrane rafts. *Nat Med* 2003;9:322–330.
32. Ito Y, Sato S, Ohashi T, Nakayama S, Shimokata K, Kume H. Reduction of airway anion secretion via cftr in sphingomyelin pathway. *Biochem Biophys Res Commun* 2004;324:901–908.
33. Guilbault C, De Sanctis JB, Wojewodka G, Saeed Z, Lachance C, Skinner TA, Vilela RM, Kubow S, Lands LC, Hajduch M, *et al.* Fenretinide corrects newly found ceramide deficiency in cystic fibrosis. *Am J Respir Cell Mol Biol* 2008;38:47–56.
34. Stiban J, Fistere D, Colombini M. Dihydroceramide hinders ceramide channel formation: Implications on apoptosis. *Apoptosis* 2006;11:773–780.
35. Son JH, Yoo HH, Kim DH. Activation of de novo synthetic pathway of ceramides is responsible for the initiation of hydrogen peroxide-induced apoptosis in hl-60 cells. *J Toxicol Environ Health A* 2007;70: 1310–1318.
36. Lang F, Foller M, Lang K, Lang P, Ritter M, Vereninov A, Szabo I, Huber SM, Gulbins E. Cell volume regulatory ion channels in cell proliferation and cell death. *Methods Enzymol* 2007;428:209–225.
37. Okada Y, Maeno E, Shimizu T, Manabe K, Mori S, Nabekura T. Dual roles of plasmalemmal chloride channels in induction of cell death. *Pflugers Arch* 2004;448:287–295.
38. Hawkins BJ, Madesh M, Kirkpatrick CJ, Fisher AB. Superoxide flux in endothelial cells via the chloride channel-3 mediates intracellular signaling. *Mol Biol Cell* 2007;18:2002–2012.
39. Fujita M, Kuwano K, Kunitake R, Hagimoto N, Miyazaki H, Kaneko Y, Kawasaki M, Maeyama T, Hara N. Endothelial cell apoptosis in lipopolysaccharide-induced lung injury in mice. *Int Arch Allergy Immunol* 1998;117:202–208.
40. Lu Q, Xu DZ, Davidson MT, Hasko G, Deitch EA. Hemorrhagic shock induces endothelial cell apoptosis, which is mediated by factors contained in mesenteric lymph. *Crit Care Med* 2004;32:2464–2470.
41. Kasahara Y, Tuder RM, Taraseviciene-Stewart L, Le Cras TD, Abman S, Hirth PK, Waltenberger J, Voelkel NF. Inhibition of vegf receptors causes lung cell apoptosis and emphysema. *J Clin Invest* 2000;106: 1311–1319.